

Influence of the use of rice husk as source of silica on the sol-gel synthesis of bioglass

M. A. Pereira^{1*}, J. E. de Oliveira¹, C. S. Fonseca¹

¹Federal University of Lavras, Department of Engineering, Lavras, MG, Brazil

Abstract

Among the agro-industrial residues, the rice husk has stood out for presenting contents higher than 90% of silica, the main oxide of bioglass. Thus, the objective of this research was to compare the use of two different sources of silica, tetraethylorthosilicate (TEOS) and rice husk ash (RHA), in the sol-gel synthesis of the bioglass of the SiO_2 -CaO- Na_2O system. For the silica extraction, the rice husk was treated with oxalic acid and calcined at 600 °C. This temperature was determined using thermogravimetry and the calcined powder was analyzed by X-ray diffraction and X-ray fluorescence spectroscopy, proving the achievement of high-purity amorphous silica. In the production of the bioglass, the solution made with the rice husk showed great synthesis efficiency, and the powder calcined was evaluated by Fourier transform infrared (FTIR) spectroscopy, Raman spectroscopy, and scanning electron microscopy. FTIR spectra presented characteristic bands of siloxane (Si-O-Si) bonds, which indicated a vitreous network and provided the formation of silanol groups, fundamentals for the growth of the hydroxyapatite layer. The microstructures of the samples were similar, but the sample made from RHA (BRHA) presented porous agglomerates, while the BTEOS had smaller and well-defined particles. The silica obtained from rice husk showed potential to be used in the sol-gel synthesis of bioglass.

Keywords: biomedical applications, electron microscopy, spectroscopy.

INTRODUCTION

The search for biomaterials that show bioactivity and bioreabsorption capacity led to the development of a material known as bioglass. The first formulation of this material was created by Larry L. Hench, in the 60s through Bioglass 45S5 with the composition 45% SiO_2 -24.5% Na_2O -24.5% CaO-6% P_2O_5 [1]. This material establishes a fast and durable chemical bond with bone tissue, through a surface of hydroxyapatite that is formed due to the release of ions between the implant and the body's physical solution [2]. Several other compositions were developed, however, the silica contents above 60% do not form a connection with the tissue, presenting a bioinert behavior [2]. This range of SiO_2 concentration can be extended by increasing the surface area that can be achieved using another synthesis methodology, such as the sol-gel process [3]. The conventional process for obtaining bioglass is melting of the components, which can have the disadvantage of evaporation of volatile components due to the high processing temperature [4]. An alternative method is a sol-gel technique, which has a low processing temperature and allows to obtain glasses with greater purity, homogeneity, and bioactivity [5-7]. This is because the sol-gel process allows greater chemical control of the surface and has fewer steps, reducing the risk of contaminations, in addition to generating products with higher surface area and porosity that are critical factors for its bioactivity [1, 4]. In addition, it is a method that allows high reproducibility and can be easily adapted from laboratory production to a large scale [8].

Silica is the main forming oxide present in a bioglass and, generally, it is obtained through alkoxy silane precursors, like tetraethylorthosilicate (TEOS), that are expensive [5]. The rice husk is a low-cost alternative source for obtaining amorphous silica, with levels greater than 90% [9]. About 23% of the total weight of the rice corresponds to the husk and it can accumulate up to 15% of silica that is stored mainly in the husk ash [9, 10]. According to CONAB, the Brazilian rice harvest 2019/20 was 11.13 million tons, generating a large volume of waste that presents slow biodegradation, due to its hard surface and high content of silicon and lignin [11, 12]. Therefore, in addition to reducing costs, the use of rice husk as a source of silica can become an interesting alternative for reducing environmental impact. In this context, the objective of this research is to analyze the effect of the use of silica obtained from rice husk in the sol-gel synthesis of bioglass of the SiO_2 - Na_2O -CaO system.

MATERIAL AND METHODS

Obtaining silica from rice husk: the rice husk (agro-industrial residue) used in this research was supplied by a processing industry in the city of Lavras-MG, Brazil. The treatment of rice husk was carried out based on a process described in the literature to obtain a high content of silica [10]. First, 40 g of husk were weighed and inserted in a beaker containing oxalic acid solution 1.2 M, in 324 mL of distilled water. The set was taken to the autoclave (mod. 104, SOC FARBE) at 1.5 kgf/cm² and 127 °C, where it remained for 1 h. After, the husk was washed with distilled water and dried in an oven at 100 °C. Differential thermal analysis (DTA) and thermogravimetric analysis (TGA) of the husk were carried out after this step to determine the calcination

*mariane.pereira1@estudante.ufla.br

<https://orcid.org/0000-0003-0399-8438>

temperature. The conditions of the analysis were heating rate of 5 °C/min up to 1000 °C, alumina crucible, and synthetic air for an approximation of working conditions. Then, the husks were calcined in a muffle with a heating rate of 5 °C/min up to 600 °C for 4 h, in an open alumina crucible and ambient atmosphere, thus obtaining the rice husk ash (RHA). For the chemical analysis of the obtained RHA, X-ray fluorescence spectroscopy (XRF, EDX-720, Shimadzu) was performed with a Ti-U analyte operating at 50 kV and 83 µA, Na-Sc analyte operating at 15 kV and 1000 µA, 10 mm collimator, and ambient atmosphere. To verify the structure of the silica obtained, crystalline or amorphous, the RHA was submitted to X-ray diffraction (XRD, SSX-550, Shimadzu). The analysis parameters were electron acceleration at 40 kV, electric current of 30 mA, and copper radiation.

Synthesis of bioglass: the bioglass was produced with the composition of 50 SiO₂-25 CaO-25 Na₂O (%mol), through the sol-gel process based on literature for the obtention of vitroceraamics from rice husk [4]. Two samples were produced, one from tetraethylorthosilicate (TEOS, Sigma-Aldrich), which has already been used commercially in the synthesis of bioglass, and the other from rice husk ash (RHA), as a source of silica (SiO₂). Two precursor solutions were produced, sodium silicate (Na₂SiO₃), by mixing the source of silica with sodium hydroxide (NaOH, Êxodo Cient.) and highly acid calcium nitrate (Ca(NO₃)₂, Êxodo Cient.) by dissolution in nitric acid (HNO₃, Êxodo Cient.). The compositions of the precursor solutions of each sample were calculated so that the components were in equal proportion and are described in Table I. The sol was formed by adding silicate solution dropwise into a highly acidic Ca(NO₃)₂ solution under a constant stirring condition to avoid gel precipitation. The pH of the sodium silicate solutions and after preparation of the sols by mixing highly acidic calcium nitrate is described in Table II. The final pH of both sols obtained indicated the desired acidic catalysts for this process. Nayak et al. [4] obtained pH 3 for the sol made from a composition similar to this work using RHA treated with HCl. The precursor sol of the BTEOS turned into a gel after 10 h at room temperature, while the precursor of the BRHA took only 30 min. This behavior was already expected due to the lower pH of the BRHA sol, which promoted a higher speed of the polycondensation hydrolysis reactions responsible for gelation. In addition, this gel was more viscous and homogeneous. The gel was aged for 48 h at 80 °C and dried for 48 h at 150 °C. The dry gel was crushed in a porcelain mortar to form a fine powder, which was calcined at 600 °C (heating rate of 5 °C/min) for 4 h

Table II - pH of sodium silicate solutions and synthesized sols.

Sample	pH of sodium silicate solution	pH of sol
BTEOS	14	4
BRHA	14	1

in an open alumina crucible and ambient atmosphere. The calcined powder was characterized by attenuated total reflectance-Fourier transform infrared spectroscopy (ATR-FTIR, MB-100C26, Boomen) and Raman spectroscopy (LabRAM HR Evolution, Horiba Sci.) for the evaluation of the formation of precursor bonds of hydroxyapatite. For this, a monochromatic green laser (532 nm) with a power of 3 mW and spectral resolution of 7 cm⁻¹ was used and for ATR-FTIR, a spectral resolution of 4 cm⁻¹. The particles formed were also analyzed for their morphology through scanning electron microscopy (SEM, LEO EVO 40 XVP, Carl Zeiss); before analysis, the samples were metalized with gold.

RESULTS AND DISCUSSION

Thermogravimetry (TGA) and differential thermal analysis (DTA) for rice husk: as can be seen in Fig. 1, there was an initial mass loss up to 100 °C of approximately 10%, which was related to the loss of physical water adsorbed on the sample and other volatile substances [11]. This endothermic event was seen in the DTA curve at 63 °C. Between 200 and 330 °C, there was a rapid and intense loss of mass of 43% linked to the thermal decomposition of hemicellulose and cellulose, which are organic components of rice husk. Hemicellulose, which is the least stable component, decomposes mainly between 200 and 260 °C and cellulose between 240 and 360 °C [13]. The exothermic peak at 315 °C indicated the decomposition of these components. The treatment of rice husks with oxalic acid allows the acid hydrolysis of hemicellulose and cellulose, making them more easily thermally degraded [14]. Between 350 and 550 °C, there was a loss of mass of about 29% due to the thermal degradation of lignin that happens between 370 and 600 °C [14]. The exothermic peak at 440 °C confirmed this phenomenon. The residue of approximately 16% was composed of rice husk ash (RHA), consisting mainly of silica. From the data of this analysis, it was decided to produce amorphous silica at a low temperature. Thus, the temperature of the calcination of the rice husk was set at 600 °C, which corresponded to the final temperature of degradation of the organic components. As verified by

Table I - Proportions of chemical reagents to prepare precursor solutions, with BTEOS made from TEOS and BRHA made from rice husk ash.

Sample	TEOS (mL)	RHA (g)	NaOH (mL)	Ca(NO ₃) ₂ (g)	HNO ₃ (mL)
BTEOS	10	0	100	12.5	50
BRHA	0	10	100	12.5	50

XRD, this treatment temperature provided the formation of amorphous silica, because it was not observed in the DTA curve an exothermic peak up to this temperature that could be associated with its crystallization. Other authors have observed a crystalline structure of silica formed from rice husk above 900 °C [14, 15].

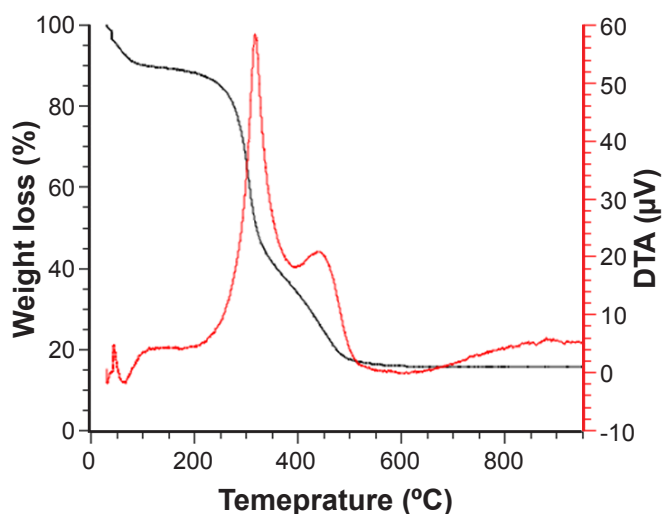


Figure 1: TGA and DTA curves of the rice husk ash (RHA).

X-ray diffraction (XRD) for RHA: the diffractogram (Fig. 2) showed the presence of an amorphous halo between $2\theta = 15^\circ$ and 31° with a maximum intensity at $2\theta = 22^\circ$, which was related to amorphous silica as predicted in the thermal analysis and similar to what was observed in other researches for rice husk calcined at 600 °C [11, 14, 15]. Both the crystalline and amorphous structures of the silica have an oxygen ion connecting two silicate tetrahedrons, although a more open arrangement is formed in the amorphous silica [16]. This open structure facilitates the inclusion of network modifying cations, mainly for amorphous silica, allowing to obtain a wide range of silica glasses [16].

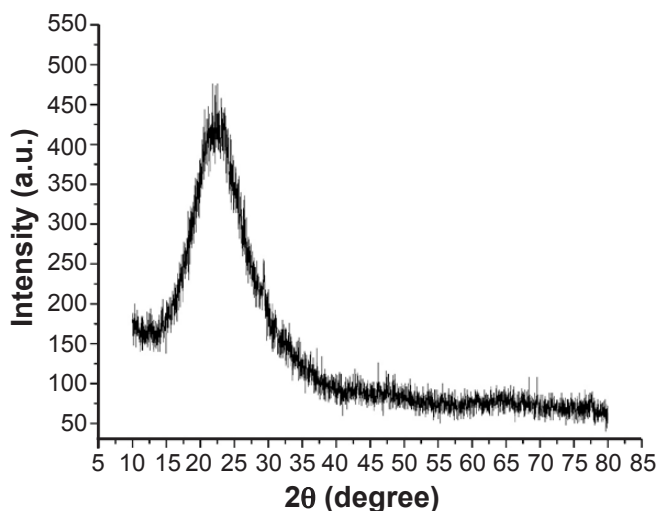


Figure 2: XRD pattern for the rice husk ash (RHA).

X-ray fluorescence spectroscopy (XRF) for RHA: from XRF, it was possible to obtain the chemical composition of the sample produced from the rice husk (Table III). The analysis showed silica as the main component, with a low amount of impurities that can also be observed in other works [11, 14, 15]. In a similar work, silica with 99.7% purity was obtained from the treatment of rice husks with oxalic acid [10]. The chemical composition of rice husk calcined at 600 °C showed SiO_2 as the major component. This result, associated with XRD analysis showed that the silica had an amorphous structure in this sample.

Table III - Chemical composition of the RHA.

SiO_2	Al_2O_3	CaO	SO_3	Eu_2O_3	K_2O
96.60	2.48	0.66	0.14	0.07	0.05

Attenuated total reflectance-Fourier transform infrared spectroscopy (ATR-FTIR) for bioglass samples: Fig. 3 shows the spectrum formed for the two samples analyzed by ATR-FTIR. Both samples showed similar spectra, with differences in the peak shape and small displacements. For the bioglass made from TEOS (BTEOS), there was a band at 1375 cm^{-1} , which moved to 1428 cm^{-1} for the bioglass made from the rice husk ash (BRHA), referring to the residual nitrate [17, 18]. Between 760 and 1044 cm^{-1} , it was possible to identify bands for the groups referring to silica like Si-O-Si and those indicating the existence of non-bridging oxygen (NBO) formed by the incorporation of the modifying ions in the silica forming network. Ca^{2+} and Na^+ ions break Si-O-Si bonds to form Si-O species present as SiO-Ca²⁺-OSi and SiO-Na⁺-OSi [17]. The absorption bands at 844, 877, and 917 cm^{-1} to the BTEOS and at 916 and 773 cm^{-1} to the BRHA were ascribed to stretching in NBO of Si-O_{NBO} [17, 19]. The band corresponding to Si-O-Si asymmetrical stretching was located at about 1040 cm^{-1} , while symmetrical stretching was detected at 617 cm^{-1} for both samples [18, 19]. The bands between 430 and 511 cm^{-1} were assigned to bending vibrations of Si-O-Si bonds in amorphous silica [19]. These bonds identified for the groups referring to silica (Si-O-Si and Si-O) provide the formation of silanol groups, which is a fundamental step for the growth of the hydroxyapatite layer when the material is placed in contact with the body fluids [20]. The interaction verified between the silica and modifying ions indicated the formation of a vitreous network. It was also observed that the BTEOS sample had slight displacements in relation to the BRHA sample, in addition to decreasing the width of the bands, which can be related to possible greater crystallinity.

Raman spectroscopy for bioglass samples: Fig. 4 shows the spectra formed for the two samples analyzed by Raman spectroscopy, which showed stretching signals corresponding to Si-O-Si bond at 840 - 1065 cm^{-1} [21]. Bands in the region of 700 to 1100 cm^{-1} are characteristic of Si-O stretching vibrations in different SiO_4 tetrahedrons, characterizing different structural units Q^n , where n is the number of binding oxygen connecting to the vitreous

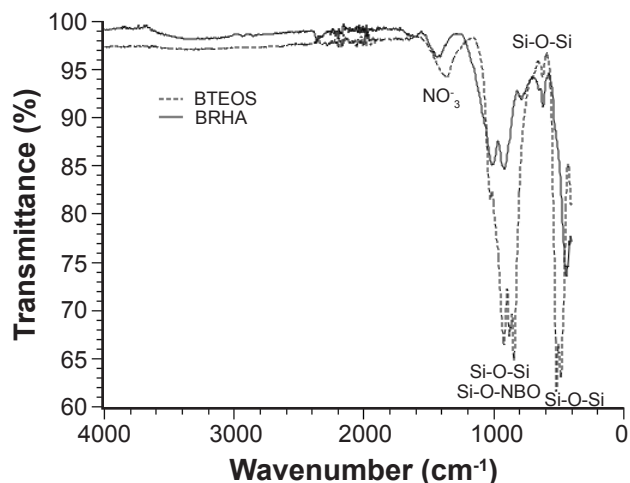


Figure 3: ATR-FTIR spectra of bioglass samples (BTEOS and BRHA).

network [22]. The intense band at about 860 cm^{-1} of the BTEOS was assigned to stretching vibrations of Q^1 silicate units and the more intense band at 980 cm^{-1} of the BRHA was assigned to vibration of Q^2 units [22]. Bands between 1000 and 1070 cm^{-1} were attributed to the asymmetrical vibrations of the Si-O-Si bonds and between 200 and 650 cm^{-1} to the vibrations of the Ca-O bond [24]. Bands between 500 to 620 cm^{-1} were observed for the two samples and corresponded to the oscillating vibration of Si-O-Si and to the small presence of Na_2O [24]. The peaks located at 420 and 1065 cm^{-1} for both samples indicated the presence of tectosilicate species, which have a 1:2 ratio of Si:O and the latter peak is characteristic of amorphous matrices rich in silica [24]. The presence of a 420 cm^{-1} band, more pronounced for BTEOS, indicated the condensation of the silanol functional group (Si-OH) to siloxane (Si-O-Si) [21]. The absence of 643 to

654 cm^{-1} bands confirmed the total hydrolysis of the starting silica [21].

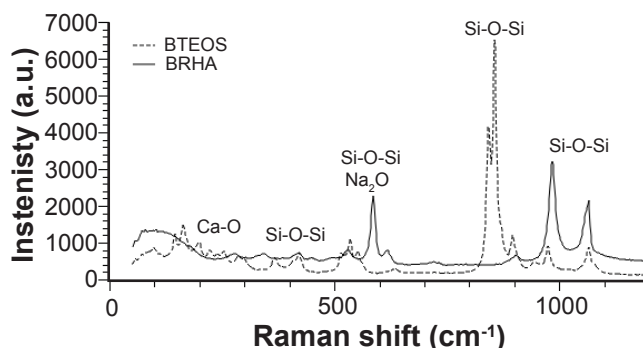


Figure 4: Raman spectra of bioglass samples (BTEOS e BRHA).

Scanning electron microscopy (SEM) for bioglass samples: the images in Fig. 5 show the microstructure and morphology of the samples. It was observed that the BTEOS morphology was more defined than that of the BRHA sample, showing itself in the form of rod clusters with irregular surfaces. Fig. 5b shows the BRHA like a porous agglomerate, but, comparing Figs. 5c and Fig. 5f with greater magnification, it is possible to note that there were particles in the BRHA sample with similar morphology to those shown by the BTEOS sample, however, with much greater dimensions and adhered to a porous surface. Other authors observed a porous structure of the bioactive material made from rice husks up to the calcination temperature of 1000 °C [5]. The porous material has advantages in the release of drugs [25]. In Figs. 5a and 5d, it is observed that the particles did not present homogeneous size and the BTEOS sample generated smaller particles. Smaller particles may favor the

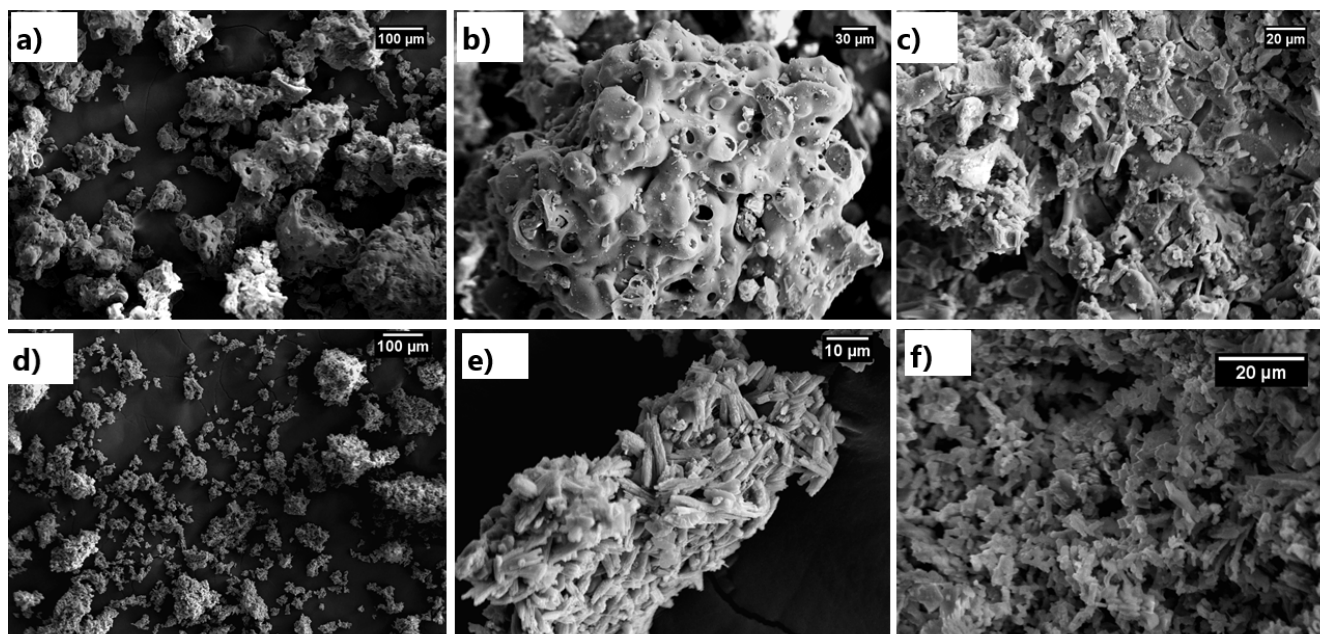


Figure 5: SEM micrographs with different magnifications of bioglass samples BRHA (a-c) and BTEOS (d-f).

formation of the hydroxyapatite layer more quickly during exposure to body fluid, due to its greater surface area of contact. This effect is beneficial for applications such as the coating of orthopedic implants and to facilitate the integration of bioglass with polymeric matrices in composites [25]. In addition, non-spherical shapes with a high aspect ratio, like the BTEOS sample, are able to adhere to cells more effectively, which is advantageous for the targeted supply of anticancer drugs [25].

CONCLUSIONS

From the calcination of the rice husks treated with oxalic acid, it was possible to obtain amorphous silica with high purity. The bioglass obtained from rice husk ash (BRHA) showed greater efficiency in the sol-gel synthesis by obtaining a more viscous gel in just 30 min. Attenuated total reflectance-Fourier transform infrared spectroscopy (ATR-FTIR) and Raman spectroscopy of the bioglass samples showed the presence of siloxane (Si-O-Si) bonds that indicated a bioactive potential of the materials because they are related to the formation stages of the hydroxyapatite layer. The powders produced from TEOS had a well-defined microstructure with smaller acicular grains, homogeneously distributed, which is beneficial for applications in orthopedic implant coatings and composites. The sample produced from the RHA, on the other hand, presented porous clusters, which is advantageous for the release of drugs. Thus, the rice husk ash showed the potential to be a source of silica in the production of bioglass.

ACKNOWLEDGEMENT

This work was supported by the Conselho Nacional de Desenvolvimento Tecnológico e Científico (CNPq-PVDCF838-2017).

REFERENCES

- [1] E.L.G. Medeiros, A.M.C. Santos, E.S. Medeiros, R.R. Menezes, *Rev. Eletr. Mater. Proces.* **12**, 3 (2017) 152.
 - [2] R.L. Siqueira, E.D. Zanotto, *Quim. Nova* **34**, 7 (2011) 1231.
 - [3] A. Lukowiak, J. Lao, J. Lacroix, J. Marie Nedelec, *Chem. Commun.* **49** (2013) 6620.
 - [4] J.P. Nayak, S. Kumar, J. Bera, *J. Non. Cryst. Solids.* **356**, 28-30 (2010) 1447.
 - [5] J.P. Nayak, J. Bera, *Appl. Surf. Sci.* **257**, 2 (2010) 458.
 - [6] V.R. Oviedo, D.M. Druzian, S.R. Mortari, M.R. Sagrillo, T.M. Volkmer, D.A. Bertuol, L.F. Rodrigues Jr., *Cerâmica* **66**, 380 (2020) 426.
 - [7] S. Cañaverall, D. Morales, A.F. Vargas, *Mater. Lett.* **255** (2019) 126575.
 - [8] I.O. Polo, D.O. Junot, L.V.E. Caldas, *J. Appl. Phys.* **125** (2019) 185102.
 - [9] N.P. Stochero, E. Marangon, A.S. Nunes, M.D. Tier, *Ceram. Int.* **43**, 16 (2017) 13875.
 - [10] L. Fernandes, M.G. Sabino, H.L. Rossetto, *Cerâmica* **60**, 353 (2014) 160.
 - [11] J.A. Santana Costa, C.M. Paranhos, *J. Clean. Prod.* **192** (2018) 688.
 - [12] Comp. Nac. Abastec., “Acompanhamento da safra brasileira de grãos”, v.1, n.1, CONAB, Brasília (2020).
 - [13] V.B. Carmona, R.M. Oliveira, W.T.L. Silva, L.H.C. Mattoso, J.M. Marconcini, *Ind. Crops Prod.* **43** (2013) 291.
 - [14] R.A. Bakar, R. Yahya, S.N. Gan, *Procedia Chem.* **19** (2016) 189.
 - [15] S.K. Hubadillah, M.H.D. Othman, A.F. Ismail, M.A. Rahman, J. Jaafar, Y. Iwamoto, S. Honda, M.I.H.M. Dzahir, M.Z.M. Yusop, *Ceram. Int.* **44**, 9 (2018) 10498.
 - [16] M. Vallet-Regí, F. Balas, *Open Biomed. Eng. J.* **2**, 1 (2008) 1.
 - [17] C.A. Bertran, O.V.M. Bueno, *Key Eng. Mater.* **631** (2014) 36.
 - [18] H.C. Li, D.G. Wang, C.Z. Chen, *Ceram. Int.* **41**, 8 (2015) 10160.
 - [19] S. Palakurthy, K.V. Reddy, S. Patel, P.A. Azeem, *Prog. Biomater.* **9** (2020) 239.
 - [20] D. Arcos, D.C. Greenspan, M. Vallet-Regí, *J. Biomed. Mater. Res. A* **65**, 3 (2003) 344.
 - [21] L.A. Quintero Sierra, D.M. Escobar Sierra, *JOM* **71** (2019) 302.
 - [22] B. Tiwari, M. Pandey, S.C. Gadkari, G.P. Kothiyal, *AIP Conf. Proc.* **568** (2013) 1512.
 - [23] C. Fredericci, D.C. Ferreira, M.C.B. de Oliveira, N.S. Pinto, *Rev. IPT Tecnol. Inov.* **1**, 1 (2016) 13.
 - [24] B.A.E. Ben-Arfa, H.R. Fernandes, I.M. Miranda Salvado, J.M.F. Ferreira, R.C. Pullar, *J. Biomed. Mater. Res. A* **106**, 2 (2018) 510.
 - [25] K. Zheng, A.R. Boccaccini, *Adv. Colloid Interface Sci.* **249** (2017) 363.
- (Rec. 30/12/2020, Rev. 04/02/2021, 26/02/2021, Ac. 03/03/2021)